JOURNAL OF GEOPHYSICAL RESEARCH, VOL. 96, NO. A6, PAGES 9595–9613, JUNE 1, 1991

The Source Location and Beaming of Terrestrial Continuum Radiation

D. D. MORGAN AND D. A. GURNETT

Department of Physics and Astronomy, University of Iowa, Iowa City

Plasma wave data from the spacecraft Dynamics Explorer 1 were used to study the source location and beaming of terrestrial continuum radiation. This study shows that the radiation usually is generated near the magnetic equator at radial distances ranging from 2.0 to 4.0 R_E. The radiation is beamed outward in a broad beam directed along the magnetic equator with a beam width of about 100°. The overall frequency of occurrence of continuum radiation was found to be 60% with a sharp increase near the midnight meridian, increasing in the dawnward direction. Several case studies are presented to illustrate various characteristics of continuum radiation. The observed characteristics are then compared with the radio window model of Jones. Several characteristics not predicted by Jones' model are observed. These include large latitudinal asymmetries, an absence of a minimum in the occurrence and intensity at the equator, a tendency for higher frequency bands to come from larger and more diffuse source regions, and the emergence of several distinct beams from a single region. In particular the absence of a minimum in the occurrence and intensity at the equator and the emergence of beams of radiation at sharply distinct angles from one source region constitute evidence against the radio window model. Also, the basic equation for the beaming angle with respect to the magnetic equatorial plane is found to be a poor predictor of the observed beaming angle. The evidence against the radio window model is partially mitigated by the facts that the source of radiation is probably extended in space and frequency and that sometimes radiation from the Sun interferes with the direction finding. Overall, these observations imply that the radio window model does not fully explain the beaming pattern of continuum radiation.

1. INTRODUCTION

In this paper the source location and beaming of escaping terrestrial continuum radiation are studied using direction-finding measurements from the Dynamics Explorer 1 spacecraft. The results are then compared with predictions of the radio window model of *Jones* [1980].

The study of terrestrial continuum radiation extends back more than 15 years. In an early spacecraft study of the galactic radio spectrum, *Brown* [1973] commented on the existence of a weak terrestrial noise source between 30 and 100 kHz. This study is frequently cited in the literature as the first detection of terrestrial nonthermal continuum radiation. However, recently *Steinberg and Hoang* [1986] presented evidence that the noise detected by Brown was a locally generated electrostatic emission, and not electromagnetic radiation. Therefore it is not clear that Brown was the first to detect continuum radiation. Shortly after the Brown report, *Gurnett and Shaw* [1973] discovered a somewhat different type of continuum radiation at frequencies of 5–20 kHz. They showed that the radiation has a magnetic field component, which proves that it is electromagnetic radiation and not a locally generated electrostatic emission. Since the frequency of this radiation is below the solar wind plasma frequency, the radiation is permanently trapped in the low-density cavity formed by the interaction of the magnetosphere with the solar wind. *Gurnett and Shaw* [1973] showed that the radiation was distributed uniformly throughout the magnetospheric cavity, apparently because of repeated reflections at the walls of the cavity. Later, *Gurnett* [1975] studied radiation at frequencies above the solar wind plasma frequency where the radiation can escape freely from the Earth, and introduced the term "escaping continuum radiation" to distinguish this radiation from the "trapped" continuum radiation. His study clearly showed that an escaping component of radiation existed at frequencies up to about 100 kHz, in the same frequency range originally reported by Brown. Using direction-finding measurements, *Gurnett* [1975] also presented evidence that the escaping continuum radiation was generated in the vicinity of the plasmapause.

The name "continuum" was originally introduced because of the diffuse, nearly continuous character of the spectrum. However, this term is not always descriptive of the spectrum, particularly at higher frequencies. *Gurnett and Shaw* [1973] point out that in some cases the trapped component of the radiation shows evidence of a banded harmonic structure, with a frequency spacing of about 1 kHz. Later, *Kurth et al.* [1981], using instrumentation with better frequency resolution, showed that the escaping radiation also had a banded frequency structure. This banded structure is sufficiently common in the escaping component that the term continuum is sometimes not appropriate. This difficulty led *Jones* [1980] to suggest that the escaping continuum should be called "myriametric" radiation, which implies wavelengths in the 10-km range. Even this terminology is not unambiguous, since in some cases the radiation has wavelengths as short as 1 km. To be consistent with our past terminology, we continue to refer to this radiation as "continuum radiation" even though the spectrum sometimes shows clear evidence of discrete band structures.

Several theories have been proposed for the origin of the continuum radiation. *Gurnett and Frank* [1976] showed that "continuum storms" occur in association with the injection of low-energy electrons into the outer radiation belts. They suggested that electrons excite electrostatic waves, which in turn produce continuum radiation via a mode conversion process. Two classes of mode conversion mechanism have been discussed: linear and nonlinear. In a series of papers spanning more than a decade, Jones and coworkers proposed that the conversion takes place via a linear mode conversion process known in the ionospheric radio propa-

Paper number 91JA00314.
0148-0227/91/91JA-00314$05.00

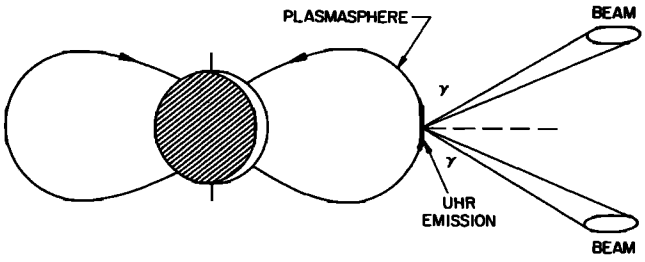

Fig. 1. Schematic diagram showing the geometry of Jones' beaming theory. The spread of the beam shows the effect of using full-wave theory and accounting for finite plasma temperature, as explained by *Jones* [1987*b*].

gation literature as the "radio window." For a description of this mechanism, see the papers by *Jones* [1976, 1980, 1981, 1982], *Lembege and Jones* [1982], *Budden* [1980], *Budden and Jones* [1987], *Jones et al.* [1987], *Jones* [1987, 1988], and *Gurnett et al.* [1988]. A discussion of the theory of linear mode conversion is also given in the textbook by *Budden* [1985]. In the process proposed by Jones, electrostatic waves near the upper hybrid resonance (UHR) frequency are converted primarily to escaping left-hand-polarized ordinary (*L-O*) mode radiation in regions of large density gradients, such as occur near the plasmapause and magnetopause [*Budden and Jones*, 1987]. According to Jones' analysis, the radiation emerges from the window in a plane defined by the magnetic field and the density gradient at two angles

$$\gamma = \pm \arctan [(f_p/f_c)^{1/2}] \quad (1)$$

relative to the magnetic field [e.g., *Jones et al.*, 1987]. The quantities f_c and f_p are the electron cyclotron frequency and plasma frequency, respectively. Since UHR waves are preferentially generated near the magnetic equator, the source of the escaping radiation is normally located very close to the magnetic equator. For a plasmapause source, the radiation is then beamed outward in two beams as illustrated in Figure 1. Jones presented data that show evidence of this beaming effect around the Earth [*Jones*, 1980, 1987] as well as at other planets [e.g., *Jones*, 1981, 1988]. The escaping radiation has also been confirmed to be propagating in the *L-O* mode by *Gurnett et al.* [1988], as predicted by Jones' theory. Since a steep plasma density gradient also exists at the magnetopause, *Jones* [1987] suggested that the magnetopause may also be a possible source region. It is clear that many features of the observations agree with Jones' theory. However, the linear mode conversion mechanism has been criticized by *Rönnmark* [1989] on the grounds that the conversion efficiency is too low to explain the observed radio emission intensities. On the other hand, a study by *Horne* [1989] suggests that the linear mode conversion process can account for the observed intensities if wave growth is integrated along the wave path.

Several nonlinear conversion mechanisms have been proposed but have not been developed as extensively as the linear radio window model [*Melrose*, 1981; *Murtaza and Shukla*, 1984]. All of the nonlinear mode conversion models involve an interaction between two waves to generate escaping electromagnetic radiation at the sum or difference of the frequencies of the two interacting waves. In almost all cases the high-frequency wave is assumed to be an electrostatic UHR wave. The second wave could be either another UHR wave or a low-frequency wave such as an ion cyclotron wave. For an overview of possible nonlinear conversion mechanisms that could account for the escaping continuum radiation, see *Melrose* [1981].

The theories of *Rönnmark* [1983] and *Murtaza and Shukla* [1984] make predictions concerning waves parallel and perpendicular to magnetic field lines. The linear theory of *Okuda et al.* [1982] and *Ashour-Abdalla and Okuda* [1984] also does not make a detailed prediction of the intensity distribution. Only the radio window theory makes a specific prediction concerning distribution of intensity with angle from the magnetic field [*Budden and Jones*, 1987]. Thus it is uniquely suited for comparison with our results.

Our main objective in this paper is to use the radio direction-finding capability of the Dynamics Explorer 1 spacecraft, hereafter referred to as DE 1, to investigate the source location and beaming of the escaping continuum radiation. Some studies of this type have already been carried out [*Jones*, 1980, 1987; *Gurnett et al.*, 1988]. However, the events presented in these papers were selected because they had characteristics that agreed with the radio window model. In this study we present a survey of all of the continuum radiation events observed in the DE 1 data set. This more comprehensive approach allows us to form conclusions based on a large number of observations, rather than on one or two isolated events that agree with a specific theory.

2. Spacecraft and Instrumentation

DE 1 was launched into an eccentric polar orbit on August 3, 1981. For a description of the spacecraft, see *Hoffman and Schmerling* [1981]. The geocentric radial distances of the apogee and perigee are 4.67 R_E and 1.11 R_E, and the orbit period is 6.6 hours. The spacecraft is spin stabilized with its spin axis oriented perpendicular to the meridian plane. The nominal spin period is 6 s.

Since continuum radiation tends to be observed at radial distances beyond 3 R_E and within about 30° of the magnetic equator, the orbit of DE 1 strongly constrains the times when continuum radiation can be observed. These times occur when the apogee is near the magnetic equator. For the DE 1 orbit, the argument of apogee advances at a rate of 108° per year. Therefore the apogee crosses the magnetic equator once every 1.67 years. During the period for which we have data, there are only two periods, roughly from January to September 1982 and from July 1983 to April 1984, for which the spacecraft was in a suitable position for studying continuum radiation. Because of this orbital constraint, the local time coverage is not uniform. Most of the observations were made in the local afternoon and evening, from about 1200 hours MLT (magnetic local time) to 0200 hours MLT.

The plasma wave instrument used to make these measurements is described by *Shawhan et al.* [1981]. All of the measurements analyzed were from the E_x electric dipole antenna, which has a tip-to-tip length of 200 m and is oriented perpendicular to the spacecraft spin axis. At high frequencies this antenna has an effective length of 100 m. For the periods of interest all of the data analyzed were obtained from a sweep frequency receiver (SFR), which samples the frequency range 100–400 kHz in 128 frequency steps with a nearly constant fractional frequency resolution. These 128

steps are divided into 4 channels of 32 steps each. In the sweep mode, each step is sampled for 1 s, so that a complete sweep takes 32 s. At the frequencies where the continuum radiation is observed, the noise level of the receiver is approximately 10^{-16} V^2/m^2 Hz.

3. Distribution in Magnetic Local Time and Correlations With Magnetic Indices

In order to determine the frequency of occurrence of continuum radiation and analyze its distribution in magnetic local time, a preliminary statistical study was undertaken. In this study the sample set consisted of spectrograms which included a spacecraft magnetic equator crossing at a geocentric distance of 3.5 R_E or greater. A distance of 3.5 R_E was chosen as the inner limit of the sampling region to assure that we would see radiation down to about 30 kHz. The events analyzed covered two periods, from February 4 to August 29, 1982, and from July 12, 1983, to March 30, 1984. The stringency of the orbit criterion has excluded some events at either end of both sampling periods.

From a total of 121 allowable equator crossings that occurred during these two periods of observation, a total of 70 continuum radiation events were identified, giving an overall frequency of occurrence of 58%. Events were identified by visual examination of the wave electric field spectrograms. A systematic examination of the magnetic field spectrogram was not undertaken because quite often the loop antenna receiver was not operating. It was almost never sensitive enough to detect the magnetic component of the continuum radiation. Another aid to identification is the upper hybrid resonance noise which is always present during continuum storms. Upper hybrid resonance noise is a very narrow band of noise seen above the electron cyclotron frequency. It often varies rapidly in frequency, indicating the passage of the spacecraft through regions of rapidly varying plasma density. Because the upper hybrid resonance is sometimes obscured by intense radio noise, it is not always visible. For this reason, it is not used as an absolute criterion for the identification of continuum radiation. The criterion for identifying escaping continuum radiation is based on its appearance, which is smooth in time, banded, and with a moirelike pattern on a spectrogram which is due to the beat frequency between the receiver sampling frequency and the spin of the spacecraft. Usually there is no confusion between continuum and auroral kilometric radiation (AKR) even though their intensity ranges overlap. AKR has fine structure that changes on a much shorter time scale than continuum radiation.

Several previous studies of the magnetic local time distribution of magnetospheric continuum radiation have been performed. *Gurnett* [1975] correlated the intensity of events with magnetic local time at 56.2 kHz (his Figure 14) and found that the most intense events occurred between 4 and 14 hours MLT. In Figure 11 of the same paper a direction-finding study showed that most of the radiation seemed to be emerging from the local morning to early afternoon. *Kurth et al.* [1981] obtained a somewhat different conclusion. Their Figure 6 shows most of the radiation emerging from magnetic local times between 0 and 6 hours MLT.

In an attempt to clarify these issues a local time study was carried out using the DE 1 data. The results are shown in Figures 2 and 3. A spectrogram was counted as a sample

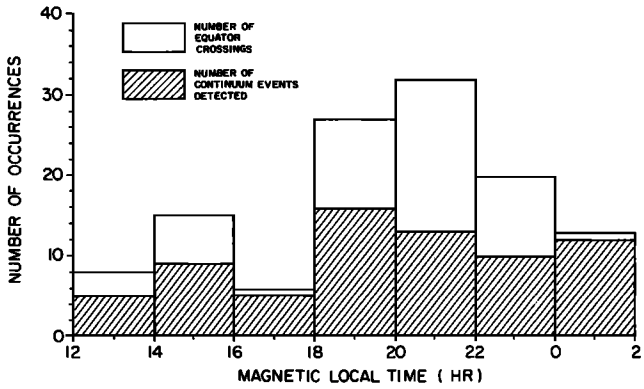

Fig. 2. Histogram showing the number of samples (unshaded) and continuum radiation events detected (shaded) as a function of magnetic local time.

when the satellite came to within 1° of the magnetic equator. Figure 2 shows a histogram that gives the distribution of samples in magnetic local time (unshaded) and the number of events detected (shaded). Figure 3 gives the frequency of occurrence as a function of magnetic local time.

Unfortunately, the findings of this study do not incorporate data from the local times where Gurnett and Kurth et al. found the highest frequency of occurrence. However, two conclusions can be made from Figures 2 and 3: (1) even during the local afternoon, when the frequency of occurrence is the lowest, the radiation seems to be present about half of the time; and (2) the frequency of occurrence reaches the highest level around local magnetic midnight. These data support the conclusion of *Kurth et al.* [1981] that the highest intensities occur in the early morning local time sector, and the data lend credence to the idea put forward by *Gurnett and Frank* [1976] that the emissions are correlated with 1- to 30-keV electrons that are injected into the magnetosphere in the local evening and drift through local midnight toward the dawnside of the magnetosphere.

An attempt was made to correlate continuum events with *AE*, *Kp*, and *Dst* indices. No consistent correlation was evident, although for several strong events, two or three of the indices were simultaneously disturbed. Using data from

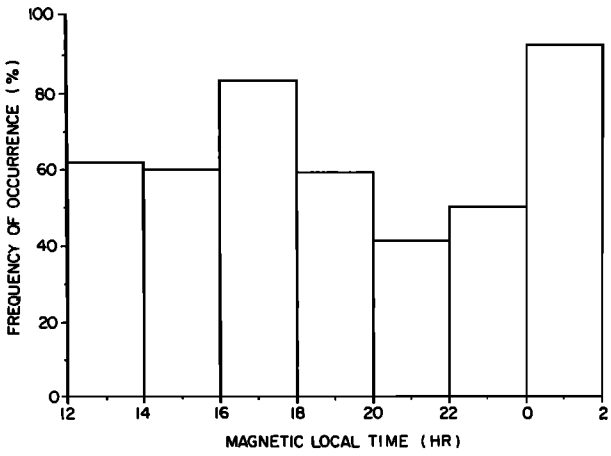

Fig. 3. Histogram showing occurrence frequency of continuum radiation as a function of magnetic local time, calculated from data shown in Figure 2.

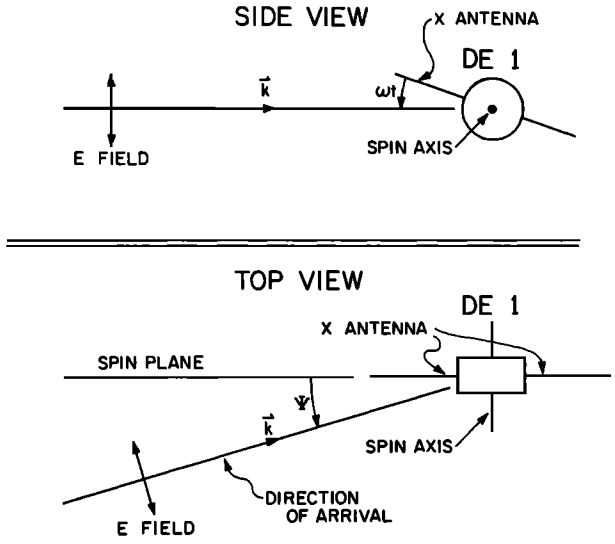

Fig. 4. Schematic diagram showing spin modulation method of direction finding. Diagram shows the case of a distant point source. Bottom panel defines the "out-of-plane" angle Ψ.

IMP 6, *Filbert and Kellogg* [1989] have published a paper since the time this work was completed showing a correlation between the *AE* index and the onset of continuum emission. A possible reason for this inconsistency is that the longer orbit period of IMP 6 enabled Filbert and Kellogg to make more precise determination of onset time than we were able to make. With the 6.6-hour orbit period of DE 1 the onset of a continuum event was more likely to be due to the spacecraft coming into position to detect continuum radiation than the physical onset of the event. Thus our temporal resolution may not have been good enough to obtain a positive correlation.

4. Direction-Finding Analysis

Because the spin axis of the DE 1 spacecraft is oriented perpendicular to the orbital plane, the E_x antenna rotates in the meridian plane of the Earth. This spin axis orientation is useful for studying continuum radiation since it provides information on source locations in the meridian plane. The direction of arrival of an incident electromagnetic wave can be determined from the spin modulation of the received signal strength. On a frequency-time spectrogram the modulation appears as a series of diagonal bands produced by the beat between the 6-s rotation of the antenna and the 32-s sweep of the SFR. These diagonal bands are easily identified in the spectrograms and permit a simple method of identifying events with spin modulation.

The direction of propagation, projected on the spin plane of the antenna, can be determined from the phase of the spin modulation pattern. For this type of analysis one assumes that the wave electric field is perpendicular to the propagation vector and that the wave is either randomly or circularly polarized. In Figure 4, ωt is the angle of the antenna axis relative to the direction of propagation (projected onto the spin plane), and Ψ is the angle of the beam from the spin plane. For the assumed field geometry, one can show that the detected electric field is given by

$$|E|^2 = |E_0|^2[1 - m^2 \cos^2(\omega t - \delta)], \quad (2)$$

where m is a number between 0 and 1 called the modulation index, and δ is the angle of the direction of arrival of the radiation from some arbitrary reference direction, most conveniently chosen to be the nadir. For a point source the modulation index m is given by $m = \cos \Psi$, where Ψ is the angle of the source out of the spin plane of the antenna (see Figure 4). For a source of finite angular size, m depends in a complicated way on the size and shape of the source [see *Baumback*, 1976]. In general, the larger the solid angle subtended by the source, the smaller the modulation index. Thus, for a modulation index less than 1, there are two interpretations: (1) the source is located outside the satellite spin plane, or (2) the source subtends a finite solid angle.

Equation (1) can be rewritten as

$$|E|^2 = A + B \cos(2\omega t) + C \sin(2\omega t) \quad (3)$$

where $A = |E_0|^2(1 - m^2/2)$, $B = -|E_0|^2(m^2/2) \cos 2\delta$, and $C = -E_0^2(m^2/2) \sin 2\delta$. Direction-finding analysis consists of least squares fitting the received power to equation (3) and using the resultant values of A, B, and C to find $|E_0|$, m, δ, and the statistic chi-squared, which is used to estimate ε, the error in δ. This method of direction finding is discussed by *Kurth et al.* [1975].

The spectrograms used for this study are stored in slide form, with a maximum of 2 hours of data on each slide. It is relatively easy to select spectrograms where the radiation has detectable spin modulation. Typical frequencies for selected events range from 3×10^4 Hz to 4×10^5 Hz (the upper limit of the spectrogram), the range for escaping continuum radiation, and bandwidth tends to be such that $0.2 \lesssim \Delta f/f \lesssim 0.4$. Times and frequencies for detailed direction-finding analysis were selected based on these spectrograms.

The next step in analyzing the data is to perform the spin modulation analysis on the chosen time and frequency intervals using a computer program. The output of this program is a plot of δ, m, and E_0 (i.e., the angle of propagation with respect to nadir, the modulation index, and the E field amplitude) versus universal time. The angle of incidence from nadir, δ, is shown with an error bar of magnitude ε, calculated from the error in the least squares fit. On the basis of this output, it is possible to select the frequency and time ranges of an event precisely. The main criterion for choosing an event was that ε be less than 5° and that the direction of arrival be smoothly and monotonically varying for four or more consecutive 5-min periods of analysis. For these events a second computer program was then used to make a diagram showing the direction of arrival of the radiation with respect to the Earth, the magnetic equator, and the spacecraft for a number of these events. The spin modulation diagrams shown in this study are the output of this second computer program.

5. Distribution of Beaming Angles

From the spectrograms and the direction-of-arrival diagrams a series of continuum radiation events was chosen for inclusion in a statistical survey of the beaming angle. There were 75 events included in this survey, 35 between January 4 and September 6, 1982, and 40 between July 19, 1983, and April 10, 1984. A histogram of these events by month is shown in Figures 5 and 6. Many of the events are multibanded, but to avoid overemphasis of any particular time

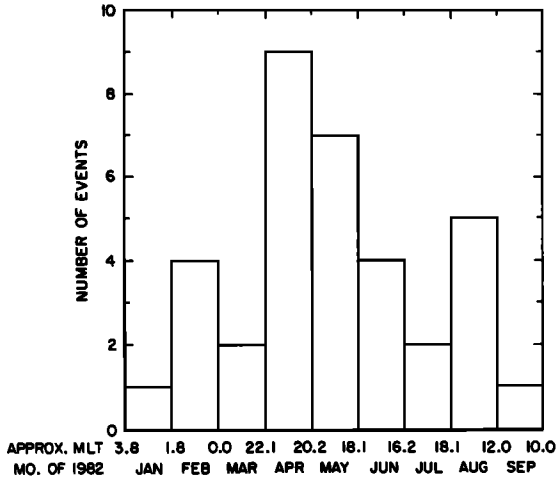

Fig. 5. Histogram showing distribution of the 35 events from 1982 used in the statistical study. The figure shows distribution by month and magnetic local time.

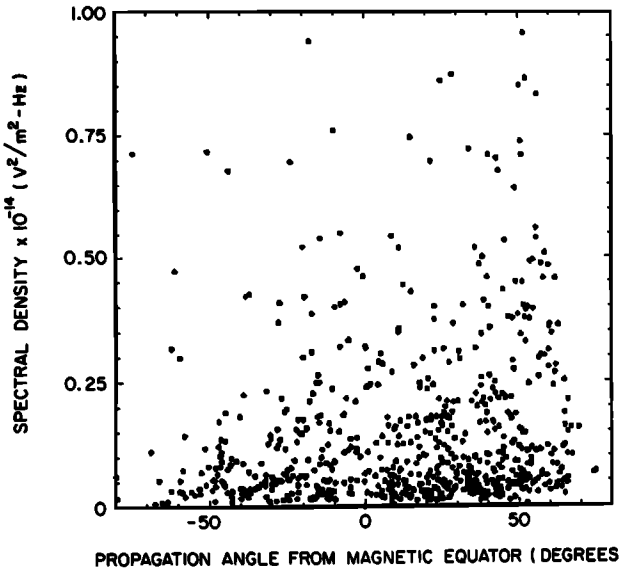

Fig. 7. Scatterplot showing received spectral density against propagation angle from the magnetic equator. Each dot represents a 5-min period of analysis.

periods, one band was chosen for each event. There was some subjectivity involved in the choice of which frequency band to use for a given event. Direction-of-arrival diagrams played a large role in deciding which band to use. Lower frequency bands were usually favored over those at higher frequencies because of their generally higher modulation index, which implies a smaller source region. But if two bands were similar in other respects, the band with the longest duration was chosen. The data were analyzed in 5-min intervals. Each of these intervals was used as a statistical unit in the analysis of beaming characteristics.

Equation (1) makes specific predictions regarding beaming geometry: a given event should have two intensity maxima symmetrically placed about the equator with a distinct minimum at the equator. To test this prediction, the intensity for all 5-min analysis intervals in the survey has been plotted against beaming angle in Figure 7. As can be seen, this plot does not show a definite reduction in intensity at or near the magnetic equator, although above 0.5×10^{-14} V^2/m^2 Hz there appears to be an occurrence gap at the equator.

If the radio window hypothesis is true, there should also be a reduction in the occurrence of continuum radiation around the magnetic equator. In order to test this prediction, the number of 5-min intervals in a given 10° angle bin was counted. A problem inherent in this type of analysis is that the spacecraft moves more slowly at distances farther from the Earth. Thus an event detected at large distances would be detected for more 5-min analysis periods than an event detected when the spacecraft was close to the Earth. To compensate for this orbit effect, each analysis period was weighted by the change in beaming angle during the analysis period. The source for each analysis period was assumed to be located at the point where the direction of arrival intersected the magnetic equator. Since it was not convenient to determine the beginning and ending points of each analysis interval, the difference in beam angle between consecutive 5-min intervals was used as the weighting factor, and the average beam angle of the two intervals was used for determining the angle bin. This simplification should not affect the result aside from a small loss in the number of analysis periods and a slight smoothing of the data. The results of this analysis are shown in Figure 8. The occurrence distribution shows a fairly uniform distribution of radiation for beam angles ranging between −40° and +40° from the magnetic equator. The minimum in occurrence expected at the equator from Jones' radio window model does not occur, although the occurrence does fall off at large angles as one would expect.

An unexpected feature of the plot in Figure 8 is the asymmetry in occurrence between the northern and southern hemispheres. The origin of this asymmetry (higher frequencies of occurrence in the northern hemisphere) is unknown. An investigation of this asymmetry indicates that the northern hemisphere peak disappears if lower-intensity events are eliminated. The histograms in Figures 5 and 6 indicate that the distribution in time of detectable continuum

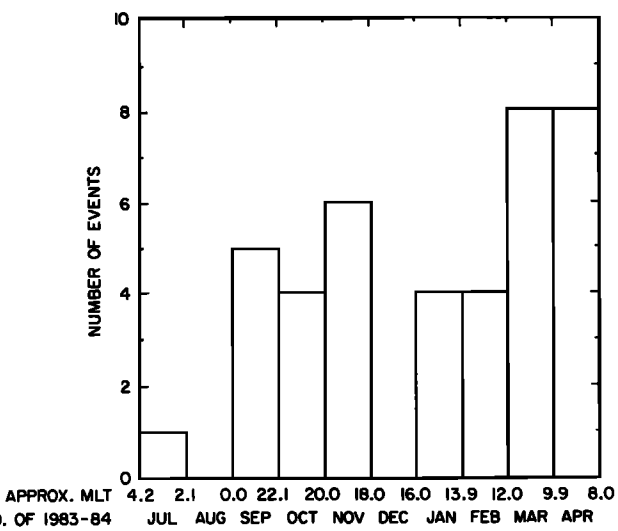

Fig. 6. Same as Figure 5 but for 40 events from the 1983–1984 period of analysis.

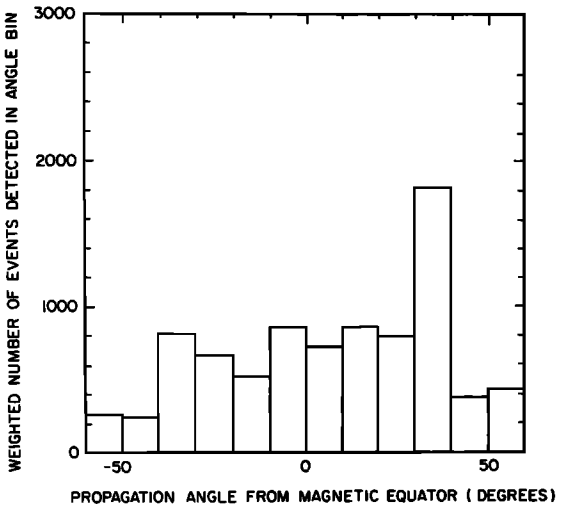

Fig. 8. Histogram showing weighted number of 5-min periods of analysis as a function of propagation angle from the magnetic equator. Each event was weighted by the number of degrees swept out by the spacecraft during the analysis period.

events can be highly variable from one period to another. Therefore it is likely that the asymmetry is simply due to random fluctuation.

6. Case Studies

The object of this section is to describe the general properties of continuum radiation, present qualitative results of this study, and illustrate those results with specific examples. The general appearance of a typical continuum radiation event is illustrated in Plate 1. The spectrogram has frequency along the ordinate and universal time along the abscissa. Several other parameters are shown along the abscissa that are functions of spacecraft position. These include the distance from the center of the Earth (in Earth radii, R_E), the L shell, the magnetic local time (in hours), and the magnetic latitude (in degrees). The spectral density of the received radiation at a given frequency and time is indicated by the color. The intensity scale is given at the right of the spectrogram. The calculated electron cyclotron frequency is labeled by f_c, and the upper hybrid resonance emission at the spacecraft is labeled by UHR. The UHR emission is identified, as described in section 3, by its narrow bandwidth and its frequency, which is usually several times the electron cyclotron frequency in this study. This basic format will be followed for all spectrograms shown in this study.

Continuum radiation is very weak and rarely exceeds electric field spectral densities of 10^{-14} V^2/m^2 Hz. For comparison, auroral kilometric radiation (AKR) often has a spectral density as high as 10^{-11} V^2/m^2 Hz. Continuum radiation often has a banded structure [see *Kurth et al.*, 1981], with typical values for $\Delta f/f$ of about 0.3. Sometimes substructure occurs with a $\Delta f/f$ of about 0.1, which is close to the resolution of the sweep frequency receiver. The emission frequency is often observed to drift on a time scale of tens of minutes, and bands of differing frequency sometimes merge with each other. No obvious pattern exists in the way in which these bands drift, nor is there any obvious explanation for why they drift. *Kurth* [1982] has shown an extremely close correspondence between "$(n + 1/2)f_{ce}$" modes, or electron Bernstein waves, and the frequency of banded escaping continuum radiation. Within the context of the radio window model, *Horne* [1990] has proposed instead that the bandedness is caused by absorption due to Landau damping at multiples of the electron cyclotron frequency.

The duration of observation of a continuum event can be anywhere from several minutes to several hours. The duration of an event is most likely limited by changes in the position of the spacecraft rather than by the physical duration of the event. It is not usual for an emission to last from one orbit to the next, putting an upper limit of 6.6 hours on the duration of most continuum events. However, during March and April 1984 there were periods when continuum radiation was continuously present for several orbits. As stated in section 1, continuum radiation is correlated with low-energy electron injections into the inner regions of the magnetosphere [*Gurnett and Frank*, 1976]. Therefore the duration of an emission should be controlled by the durations of the transient electron injections. During continuum radiation events, strong emissions are often observed at the upper hybrid frequency, f_{UHR}, which is given by the formula

$$f_{UHR} = (f_p^2 + f_c^2)^{1/2} \tag{4}$$

where f_p is the electron plasma frequency and f_c is the electron cyclotron frequency. In the region traversed by the spacecraft, $f_p \gg f_c$, so that

$$f_{UHR} \approx f_p = 9(n_e)^{1/2} \text{ kHz} \tag{5}$$

where n_e is given in particles per cubic centimeter. The onset of a continuum radiation event is often accompanied by a visible drop in the local f_{UHR}. This drop in f_{UHR} is caused by the spacecraft crossing the plasmapause into a region of lower plasma density. The plasma frequency acts as a propagation cutoff for the continuum radiation.

An important topic to be studied is the dual beam symmetry of continuum radiation with respect to the magnetic equator. The model of Jones predicts such symmetry. Unfortunately, there is only one case of which we are aware that exhibits a symmetric dual-beam structure: the case of May 6, 1982, analyzed by *Jones et al.* [1987]. Figure 1 of their paper shows two distinct intensity maxima located symmetrically with respect to the magnetic equator. The angular distribution of these maxima was shown to be consistent with the radio window theory put forward by Jones. A somewhat more typical event is analyzed by *Gurnett et al.* [1988]. Plate 1 of their paper shows two distinct maxima on opposite sides of the magnetic equator with a clear frequency shift between them. A study of the circular polarization of these two maxima is in agreement with the predictions of Jones' theory. In explaining the frequency shift, Gurnett et al. assumed that the continuum radiation is generated in regions with $f_{UHR} \simeq (n + 1/2)f_{ce}$, where n is an integer. The source of radiation was then presumed to have moved to a region in which the coincidence of $(n + 1/2)f_c$ and f_{UHR} took place at a lower frequency.

Both of these previously analyzed cases show distinct maxima arranged more or less symmetrically about the magnetic equator. However, as will be shown in this paper, neither the symmetry nor the existence of distinct intensity maxima can be taken for granted. Furthermore, many events comprise several radiation bands over a wide frequency

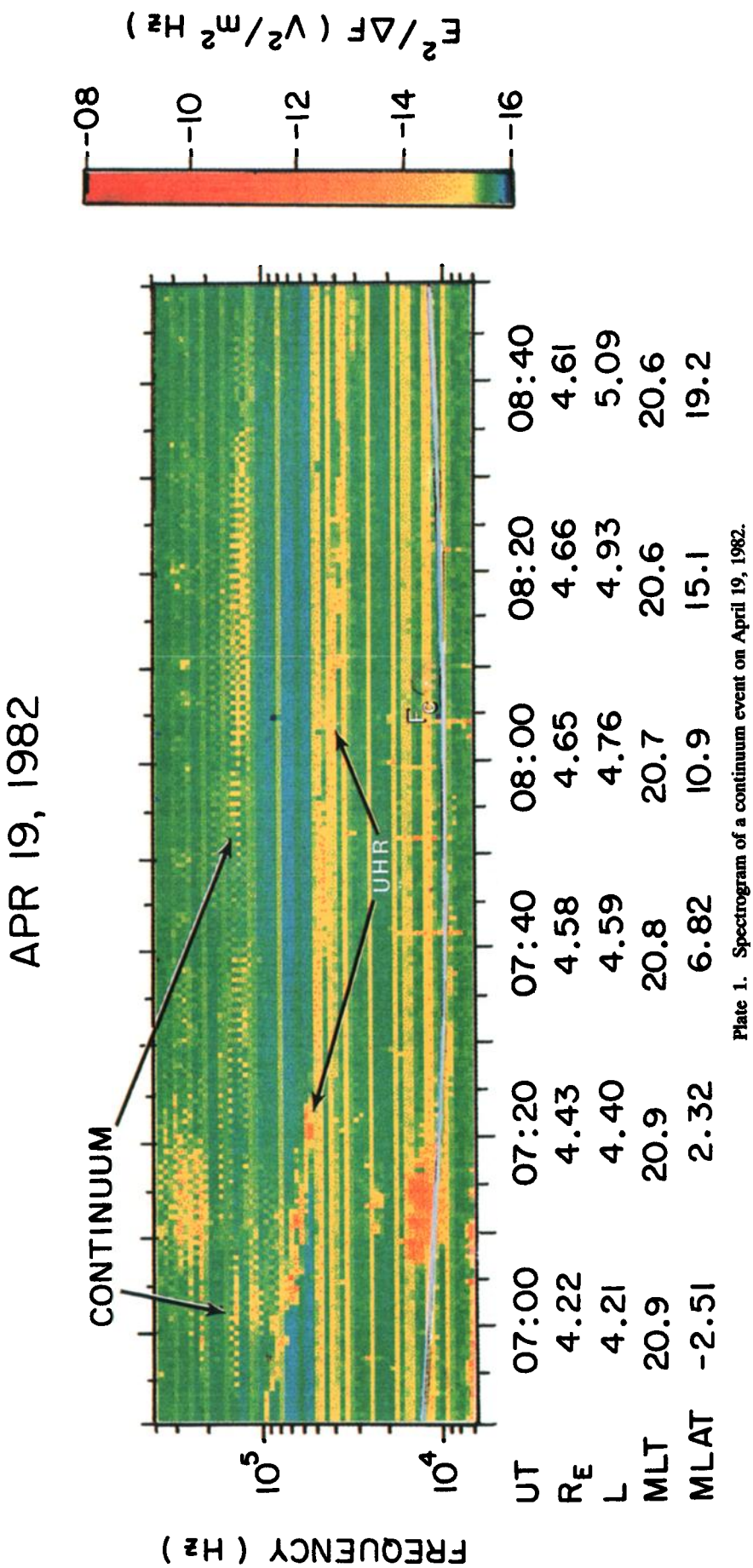

Plate 1. Spectrogram of a continuum event on April 19, 1982.

range, and these bands exhibit different source characteristics.

The aspect of continuum radiation that is most directly addressed by this study is the location of the source. In attempting to locate the source of the radiation, it is difficult to separate bands of radiation because of the way the different frequency bands shift and mingle with each other. However, certain trends are evident: higher-frequency sources appear to be closer to the Earth, have lower spin modulation indices, and are progressively more spatially extended than lower-frequency sources. Thus the source region is apparently larger and more diffuse at higher frequencies than at lower frequencies. The radiation at higher frequencies is also sometimes seen at frequencies around the first harmonic of a lower-frequency emission. Finally, at very high frequencies the continuum radiation sometimes fades into a very faint wideband radiation apparently coming from the sunward direction. This radiation is probably of solar origin and is unrelated to the continuum radiation.

The location of the source is a problem that will be seen to imply different solutions for different cases. Almost all cases in this study appear to have their primary sources at or near the plasmapause and close to the magnetic equator. However, in most cases the modulation index decreases with increasing frequency. This dependence indicates that the source broadens as the frequency increases. The physical direction of the source broadening is unclear: it could be extended along the magnetic equator or along a magnetic field line, or in both directions.

The following several paragraphs will be devoted to describing specific examples of continuum radiation. These examples are chosen to illustrate the aspects of continuum radiation noted in the previous several paragraphs, particularly concerning the change in the direction-of-arrival pattern with change in the frequency of the radiation band. Other noteworthy properties will also be discussed.

The event shown in Plate 1 is faint even for a continuum radiation event since its spectral density does not go above about 10^{-15} V^2/m^2 Hz. The event begins with the upper hybrid frequency falling from 100 to 50 kHz over the period 0650–0730 UT. Above 200 kHz a banded type of radiation is visible between 0700 and 0740 UT. Although this radiation looks similar to continuum radiation, it exhibits no consistent spin modulation. This type of radiation was observed in at least one other case in association with continuum radiation. After 0740 UT this radiation fades out into what may be AKR.

Between 100 and 200 kHz, strongly spin-modulated radiation exists for the duration of the event. The spin nulls are plainly visible. The radiation starts out in two distinct bands. However, by 0730 UT the two bands have merged, and the most intense part of the radiation appears as a single undifferentiated band for the remainder of the event. It should be noticed, however, that there are faint components of the emission around and below 100 kHz between 0655 and 0730 UT and between 0830 and 0850 UT.

The radiation is not smooth in time. There are noticeable breaks in the intensity at 0720, 0742, 0759, and 0835 UT. These breaks are accompanied by what appear to be changes in the frequency structure. At 0720 the lower-frequency component fades out, and the bands between 100 and 200 kHz begin to merge. By 0742 UT the merging is complete, and this band is sharply reduced in intensity. Between 0750 and 0759 UT there is a small enhancement which breaks off. It immediately begins again, this time at a slightly lower frequency until it breaks off at 0835 UT. At this point, the emission below 100 kHz has begun again. The emission is not symmetric about the magnetic equator. It is not centered on the magnetic equator, and no other lines of symmetry are apparent. The lack of latitudinal symmetry could be related to the position of the spacecraft. The UHR frequency is observed to drop at about the time the continuum switches on; therefore the asymmetry is not indicative of an intrinsic asymmetry of the beaming pattern. Between 50 and 100 kHz there is a band of radiation that switches on at 0700 UT, switches off again at 0720 UT, switches on at 0830 UT, and is still on at 0850 UT, where the spectrogram ends.

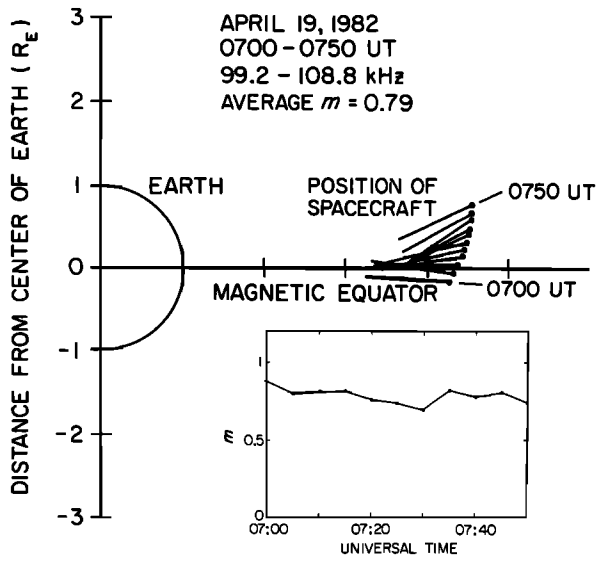

Fig. 9. Direction-finding result for a component of the continuum radiation event shown in Plate 1.

Figure 9 shows an example of the direction-finding diagrams used in this study. In these diagrams the Earth is shown as a semicircle at the left, and distances are marked in Earth radii (R_E). The horizontal axis represents the magnetic equator, and the spacecraft position is indicated at 5-min intervals by solid dots. If a dot is missing, it is because the calculated direction of arrival has an error of greater than 5°. The time and frequency ranges, as well as the average spin modulation index (m), are indicated on the diagrams. The inset shows the modulation index as a function of universal time. A larger dot is used where the error in the direction of arrival exceeds 5°. This format will be followed for all direction-finding diagrams in this study. Direction-finding diagrams will in some cases be accompanied by graphs of m against universal time.

Direction-of-arrival diagrams of the two major bands of radiation between 100 and 200 kHz and between 0700 and 0750 UT are shown in Figures 9 and 10. For the lower band shown in Figure 9, a very definite source is seen at 3.7 R_E, exactly on the magnetic equator. As the radiation dies out, the directions of arrival break away from the source. After about 0750 UT the radiation is too faint to give a good direction. The spin modulation index m as a function of universal time is shown in the inset to Figure 9. The modulation index m is somewhat erratic and averages 0.79.

For the upper band the continuum radiation was analyzable across the entire spectrogram. The direction-finding results are shown in Figure 10, and m is shown in the inset. Note that in spite of the visible variation in intensity of the radiation, m is quite stable, averaging 0.87. There is a source located at 3.5 R_E, again almost exactly on the magnetic equator. However, at 0730 UT the directions of arrival undergo a transition: they can be interpreted as coming from a source on the equator extended around 3 R_E or as emanating roughly perpendicular to a magnetic field line. It is not obvious which of these alternatives provides the best interpretation.

Figure 11 shows the two low-frequency components at 0700–0720 UT and 0830–0845 UT. If ray paths are traced back to the magnetic equator, then the radiation appears to come from two very distinct sources. Between 0705 and 0740 UT the source is virtually identical to that at slightly higher frequencies at the same time, shown in Plate 1. Between 0830 and 0845 UT the source is in the same position as that between 0730 and 0835 UT in Figure 10. To sum up this event, the band of radiation between 99 and 109 kHz gives the most definite source position. The upper radiation band between 134 and 139 kHz shows m to be very stable. Between 0735 and 0830 UT, ray paths cross the magnetic equator in a range between 2.8 and 3.3 R_E. However, it is also possible to construe the source of this radiation as being extended either along a field line or along the magnetic equator. The lower component of radiation between 80 and 100 kHz fades out at about 0730 UT and fades in again at about 0830 UT. The directions of arrival, if traced back to the magnetic equator, indicate two distinct source regions at 2.8 and 3.8 R_E, close to the magnetic equator.

Plate 2 shows a spectrogram of a strong event on January 30–31, 1984. This event exhibits three distinct bands: 40–50 kHz, 50–100 kHz, and 120–170 kHz. The highest frequency band is much fainter than the lower two. The lowest band lies on top of a sharp cutoff, probably the electron plasma frequency in the neighborhood of the spacecraft. This band fades to zero intensity before the magnetic equator is reached and exhibits an upward frequency trend. Direction-finding results and the modulation index for the 40- to

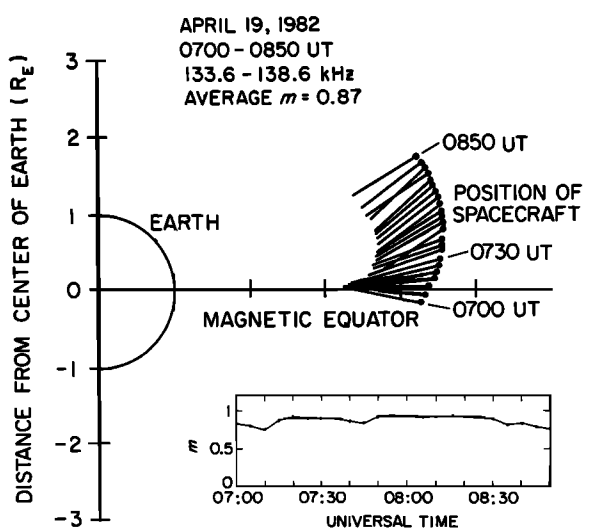

Fig. 10. Direction-finding result for the high-frequency component of the continuum radiation event shown in Plate 1.

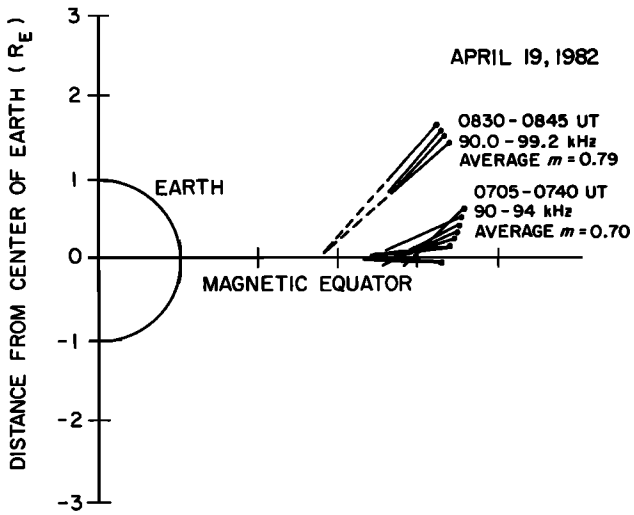

Fig. 11. Direction-finding result for low-frequency components of the continuum radiation event shown in Plate 1. These low-frequency components appear to switch off and then on.

50-kHz band are shown in Figure 12, with the modulation index m shown in the inset. They show a point source located near the magnetic equator (at 3.8 R_E) and a consistently high modulation index of $m \simeq 0.92$.

The 50- to 100-kHz band is extended in both directions about the magnetic equator. This band has an upward frequency trend with decreasing magnetic latitude. Figure 13 shows direction-finding results for this band with modulation index again shown in the inset. The pattern is not symmetric about the magnetic equator. A slight intensity minimum at the magnetic equator separates two regions which appear to come from distinct sources: rays south of the magnetic equator which come from a source at ~2.8 R_E, and rays north of the magnetic equator which come from a source at ~3.3 R_E. Both of these sources are located near the magnetic equator. This result is similar to the result found by *Gurnett et al.* [1988] for the event of March 2, 1982. The average modulation index for this band is $m \simeq 0.91$, slightly lower than for the 40- to 50-kHz band.

Direction finding for the highest frequency band is shown in Figure 14. This band is visible on the spectrogram in Plate 2 from 120 to 170 kHz as two intensity maxima roughly symmetric about the magnetic equator. This faint band of radiation exhibits considerable frequency structure. The maximum on the right, centered at about 0030 UT, shows two distinct frequency subbands. The lower subband, fairly broad in its bandwidth, appears to be associated with some enhancements that look like harmonics of the electron cyclotron frequency. There is no source visible in the spectrogram for the highest frequency band. Viewed as a whole, this band of emission has a general downward frequency trend, in conflict with the other two bands.

Figure 14, which shows the direction-finding diagram of the highest frequency band, shows a pattern that is very similar to the middle frequency band. The major difference is that the ray paths do not converge as sharply. The modulation index for this band is also significantly smaller. North of the magnetic equator there is another source interfering with the direction of arrival. Ignoring these two rays, it is clear that the directions of arrival are not converging as sharply as

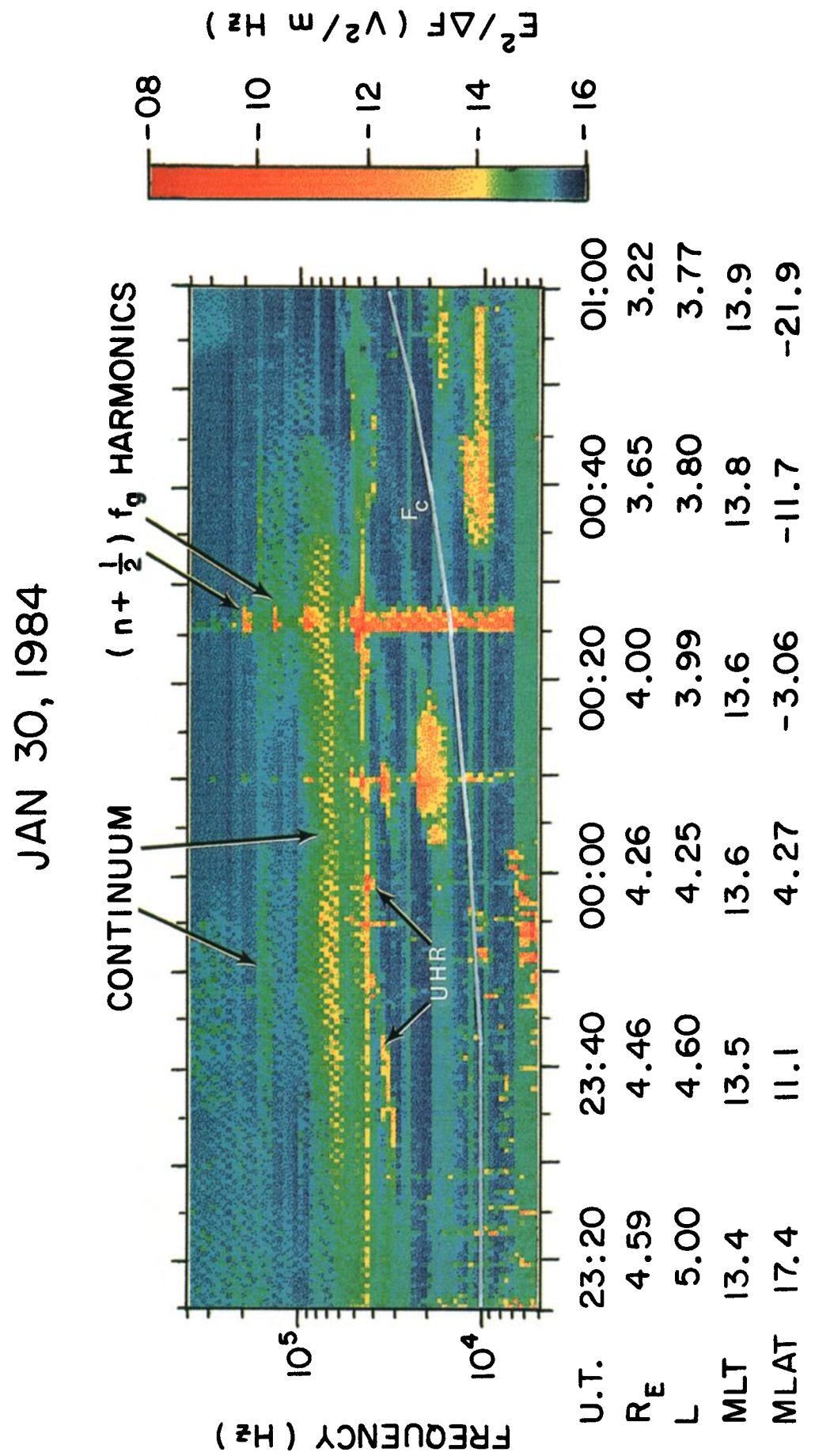

Plate 2. Spectrogram of a continuum event on January 30–31, 1984.

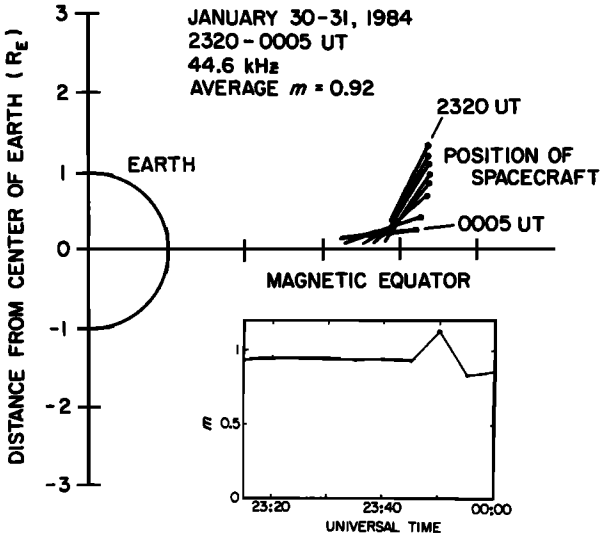

Fig. 12. Direction-finding result for lowest frequency band of continuum radiation event displayed in Plate 2.

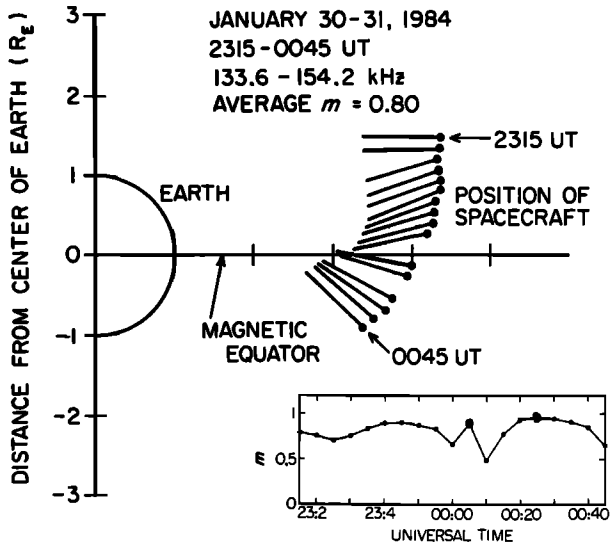

Fig. 14. Direction-finding result for the highest frequency band of the continuum radiation event shown in Plate 2.

they do for the lower frequency, indicating a larger source region. This conjecture is supported by the average modulation index for the three bands: $m \simeq 0.92$, 0.91, and 0.80 from lower to higher frequency, respectively. Note that the upper band is at about twice the frequency of the middle band. At frequencies higher than the upper band the faint radiation that is visible appears to come from the sunward direction. This radiation probably originates from the Sun and is unrelated to the event being studied.

To sum up this event, the following characteristics are seen: a complex banded structure, a partial symmetry with respect to the magnetic equator, and an increase in angular size of the source with increasing frequency. The asymmetry appears to be associated with a change in source position as well as shifts in the frequencies of the radiation bands.

Plate 3 shows a continuum event that took place on February 23, 1982. This event has three easily discernible bands of radiation running straight across the spectrogram.

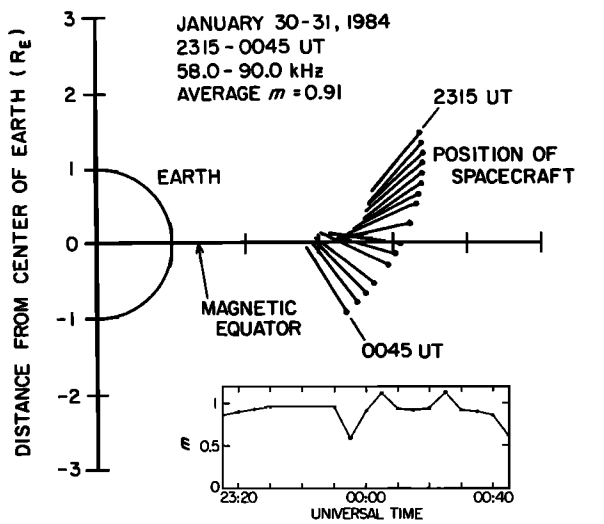

Fig. 13. Direction-finding result for the middle frequency band of the continuum radiation event shown in Plate 2.

These bands are at roughly 30–40 kHz, 40–50 kHz, and 50–70 kHz. A general upward frequency shift in the lower two bands is plainly visible while the upper band fades in intensity.

Figure 15 shows the analysis of the lowest frequency band at 30–40 kHz. The directions of arrival converge very tightly. Figure 16, for the middle band, shows directions of arrival that do not converge quite as strongly. The result is similar in form to Figure 15, but the directions of arrival are distinctly different. Finally, Figure 17 gives the highest band, 50–70 kHz. This band is different in character from the other two. It does not display a marked convergence, and the angle with respect to the magnetic equator appears to be constant. The average distance at which it crosses the magnetic equator is $\sim 2.4\ R_E$. Some variation appears to be attributable to the 40- to 50-kHz band shifting upward in frequency and encroaching on the frequency of the upper band. The rays do not converge well. Nonetheless, they display a definite angle with respect to the magnetic equator. The modulation indices in these three cases average $m \simeq 0.94$, 0.93, and 0.76, indicating that the highest frequency band has a different character from the other two bands. Note that this band is at about twice the frequency of the lowest band. Thus, as in the previous event, two low frequency bands are similar in form while a third, high frequency band has a qualitatively different appearance.

Plate 4 shows a spectrogram of the very strong event of April 4–5, 1984. This event occurred in the midst of a period of intense and frequent continuum activity between March 30 and April 10, 1984. It is one of the strongest events recorded and is very similar in its form to the event of March 2, 1982, analyzed by *Gurnett et al.* [1988]. Harmonics of the cyclotron frequency are easily visible near the magnetic equator. There are two very bright maxima extending for about 20 min on either side of the magnetic equator. A careful inspection of the spectrogram shows that these maxima make contact with different cyclotron frequency harmonics, although they are at about the same frequency. The general upward trend of the cyclotron frequency harmonics corresponds to the increase in the cyclotron fre-

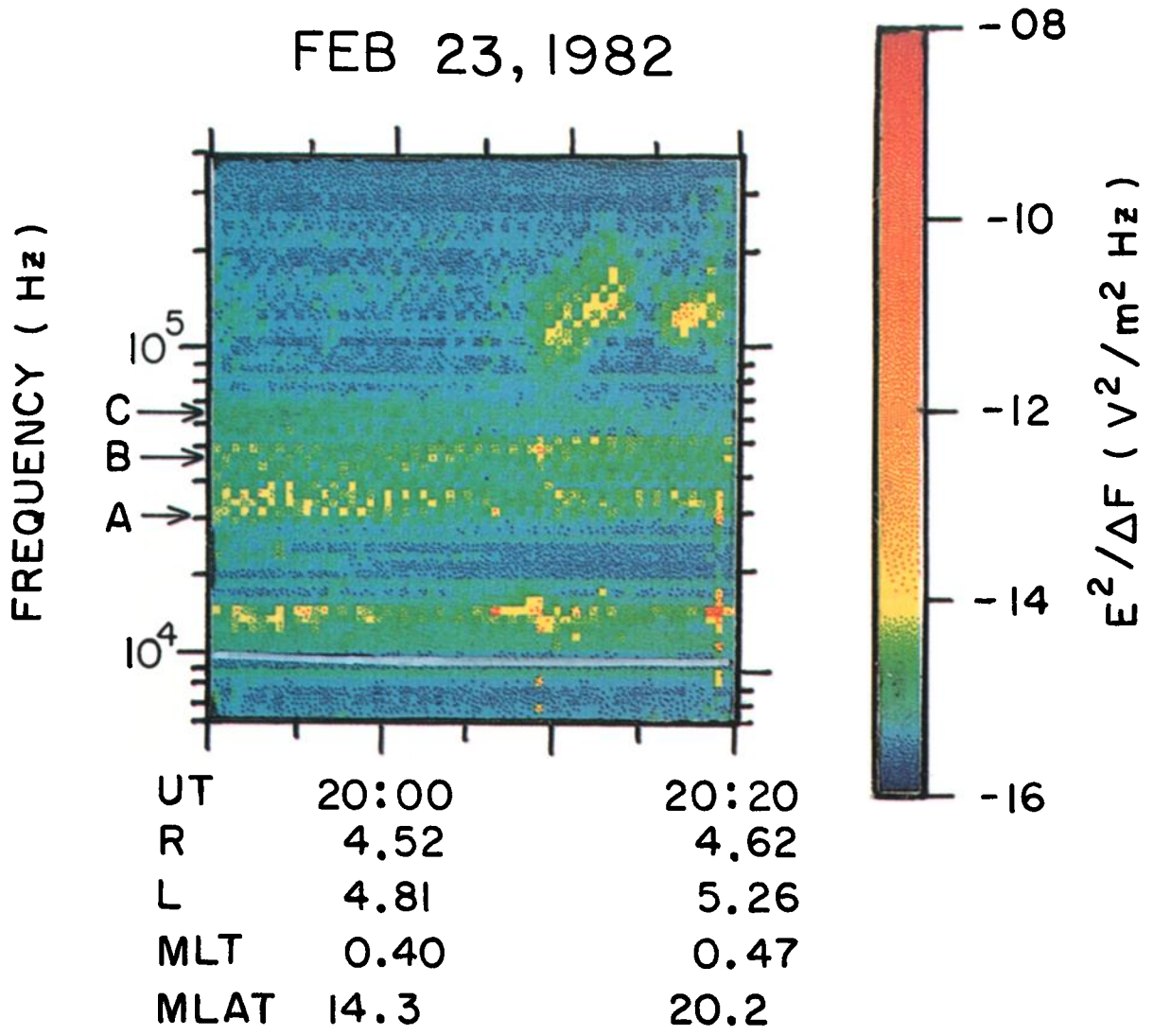

Plate 3. Spectrogram of the continuum radiation event of February 23, 1982, between 1950 and 2020 UT. There are three distinct bands of radiation: 28–35 kHz, 40–50 kHz, and 50–70 kHz.

quency and to the motion of the spacecraft to regions of higher magnetic field.

In addition to the very bright areas, there is a less bright band ($\sim 10^{-12}$ V^2/m^2 Hz) that extends up to about 100 kHz. If spin modulation analysis is carried out on the 71-kHz band all the way across the spectrogram, the transition between this band and the very bright band encroaching on it is visible. This analysis was carried out, and the result is in Figure 18.

One reason that this diagram is interesting is that the break between the fainter, higher-frequency source and the brighter, lower-frequency source is clearly visible at about 0010 UT. There is an abrupt change of about 5° in the direction of propagation. Thus the different bands are clearly propagating at different angles. What makes it even more interesting is that the three beams appear to come from approximately the same region along the magnetic equator. The implications of this fact will be discussed in section 7.

Plate 5 shows a case from August 1, 1982, in which two distinct intensity maxima appear from 1840 to 1855 UT and from 1900 to 1910 UT, respectively. The latter intensity maximum displays an upward trend in frequency with increasing magnetic latitude. At a slightly higher frequency there is a strong AKR event. At 1840 UT this event has a sharp low-frequency component that appears to be related to the observed continuum radiation.

Figure 19 gives direction-finding results for a band of radiation across the high-intensity part of the event. Some of the ray paths converge at about 4 R_E from the center of the Earth and 12° north of the magnetic equator. As the spacecraft moves northward, the directions of arrival become roughly parallel to each other and might be construed to come from a source distributed in latitude along a magnetic field line. This pattern is the same as that of the April 19, 1982, event as shown in Figure 10, except that the point of convergence is not on the magnetic equator.

From the observations and analysis described in this section, it is possible to make the following statements about continuum radiation.

1. Continuum events that explicitly display a two-beam geometry are very rare.

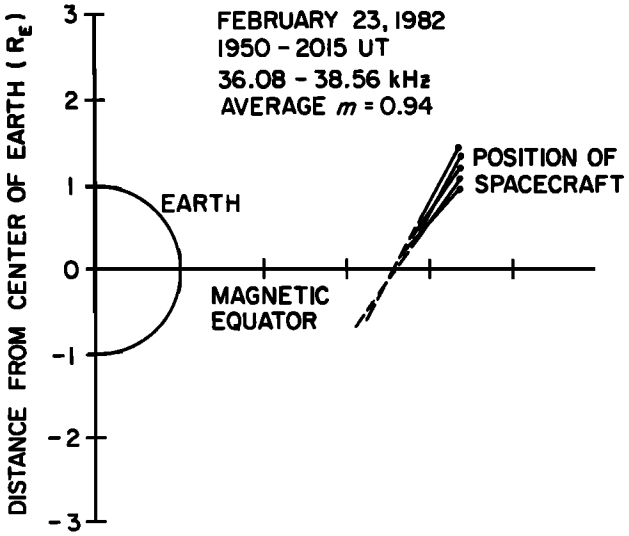

Fig. 15. Direction-finding result for the lowest frequency band of the continuum radiation event shown in Plate 3.

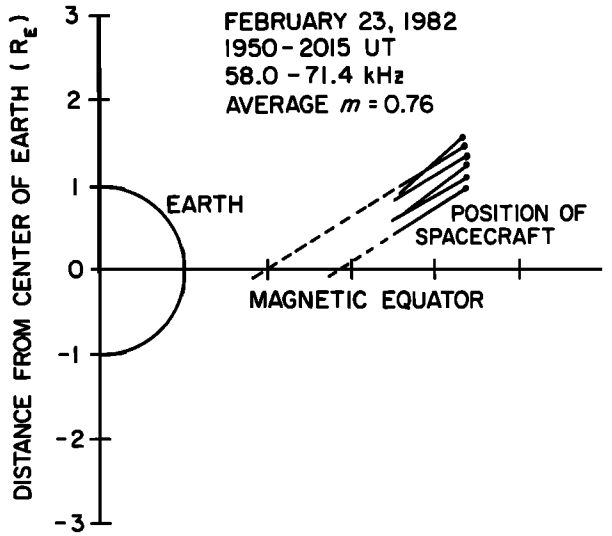

Fig. 17. Direction-finding result for the highest frequency band of the continuum radiation event shown in Plate 3.

2. Continuum events that display symmetry about the magnetic equator are rare.

3. A typical continuum event can comprise several frequency bands and spread over several hundred kilohertz. These bands are sometimes observed to shift in frequency and merge with each other.

4. At low frequencies there is typically a well-defined source radiating into a large range of angles ($\lesssim 50°$) in the meridian plane.

5. At higher frequencies the source of radiation tends to be more diffuse than at lower frequencies, and it gives a lower spin modulation index.

6. Sometimes harmonics of a given radiation appear to be excited. These harmonics have lower intensities, significantly lower spin modulation indices, and much more poorly defined sources than do the "parent" emissions.

7. Occasionally a source of continuum radiation occurs that is well away from the magnetic equator. These events appear to be associated with auroral kilometric radiation.

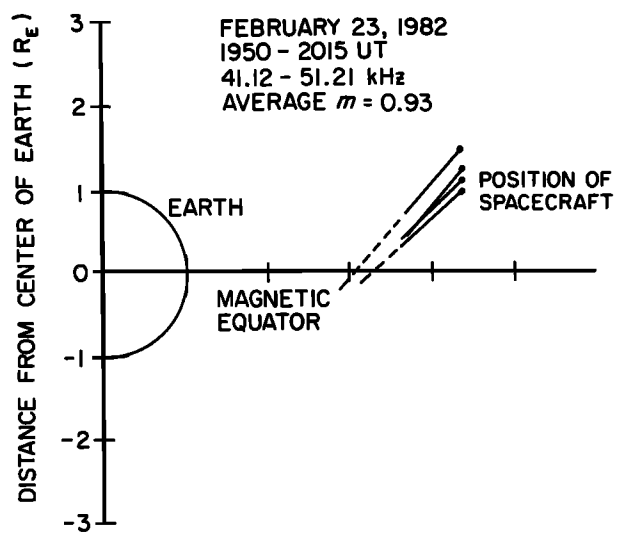

Fig. 16. Direction-finding result for the middle frequency band of the continuum radiation event shown in Plate 3.

7. Discussion

In this study, a number of properties of continuum radiation have been observed and analyzed. We will now compare these observations with the predictions of the radio window hypothesis of Jones and others.

The predictions of the radio window hypothesis in its simplest form are as follows: a source point along the magnetic equator should give rise to two beams at equal angles from the magnetic equator as given by equation (1). The inclusion of warm plasma effects and the use of a full-wave theory broaden the longitudinal extent of the beam but do not change the latitudinal intensity profile (see Figure 4 and the bottom panel of Figure 8 of *Budden and Jones* [1987]). Furthermore, since the radio window mechanism is efficient only in a region in which ∇N_e is nearly perpendicular to **B**, the source should be at the magnetic equator except in times of strong magnetic disturbance. A basic feature of the source geometry is its symmetry. The radiation is generally expected to be symmetric about the magnetic equator.

To get a better idea of the predictions of the radio window hypothesis, it is useful to use equation (1) in conjunction with a model of the electron plasma frequency. This was done for two of the individual cases studied, January 30, 1984, and April 4, 1984. The electron density models are based on averages of sets of electron data corresponding to the specified geomagnetic conditions and were provided by R. R. Anderson. One result of this calculation is shown in Figure 20 for the January 30, 1984, event. This figure shows direction of radiation from point sources on the magnetic equator in the range in which such sources are observed in this study. The number associated with each source point is the plasma frequency in kilohertz at that point calculated from the model. This diagram shows that in spite of a wide variation in source geocentric distance and frequency the beaming angle is fairly constant. The same result is found in the case of April 4, 1984. A comprehensive comparison of

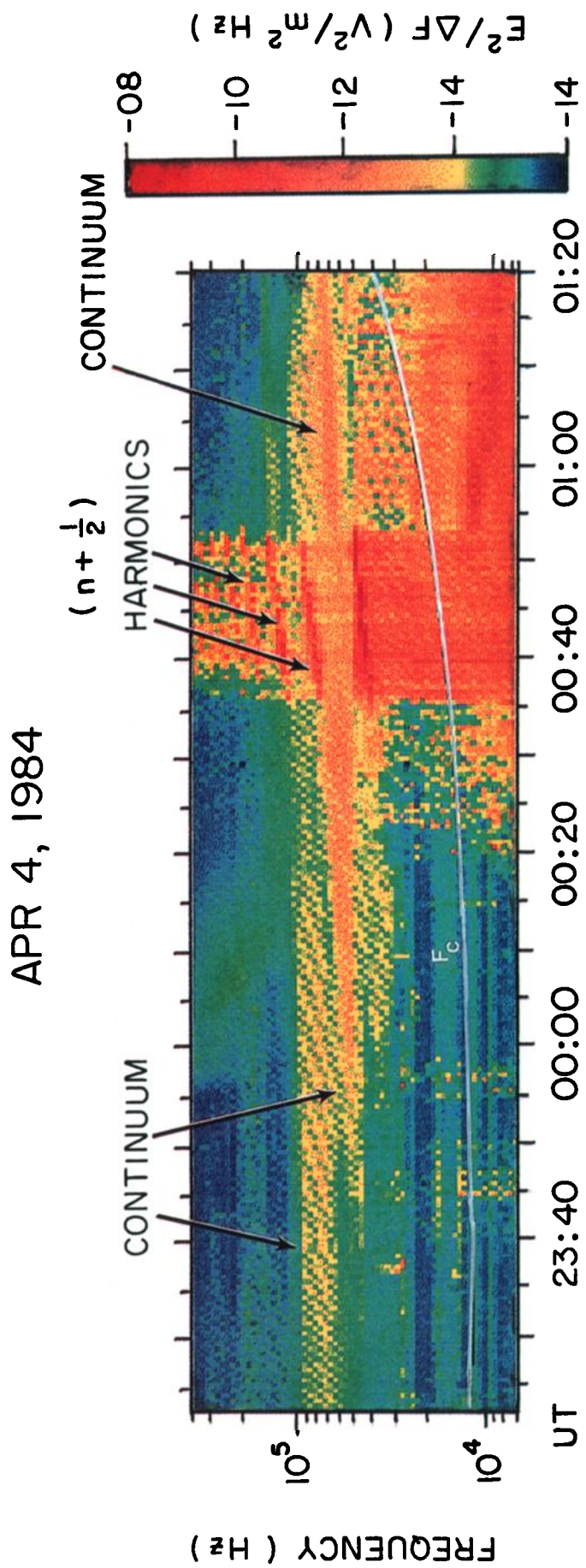

Plate 4. Spectrogram of the continuum radiation event of April 4–5, 1984. Notice the very bright component at 70–80 kHz and the fainter band up to 100 kHz.

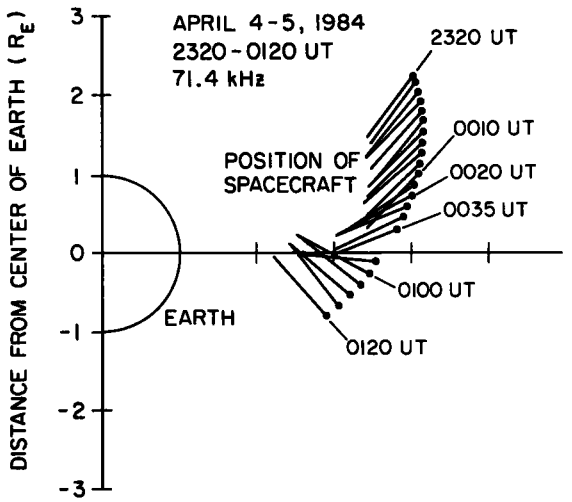

Fig. 18. Direction-finding results for the continuum event of Plate 4. Notice changes in direction of arrival at 0010 UT and 0055 UT corresponding to changes in the band of radiation detected.

measured beaming angles with calculations using reliable electron density models needs to be done, but these two cases indicate that wide variation in beaming angle should not be seen and that the beaming angle should always be around 20°.

Even without using a model of the electron density it is possible to do a comparison of these results with the predictions of equation (1). Virtually all continuum events have their sources near the magnetic equator between 2.0 and 4.0 R_E geocentric distance and occur at frequencies between 30 and 200 kHz. These parameters give limits on the beaming angle of 20° and 60°. Again, we should see little radiation at angles less than 20° from the magnetic equator.

Finally, specific beaming angles can be compared with the predictions of (1) using frequency and source position from the direction-finding diagrams and spectrograms. A number of calculated and observed beaming angles are tabulated in Table 1.

The prediction that the beaming pattern should be symmetric about the magnetic equator is not born out by a casual

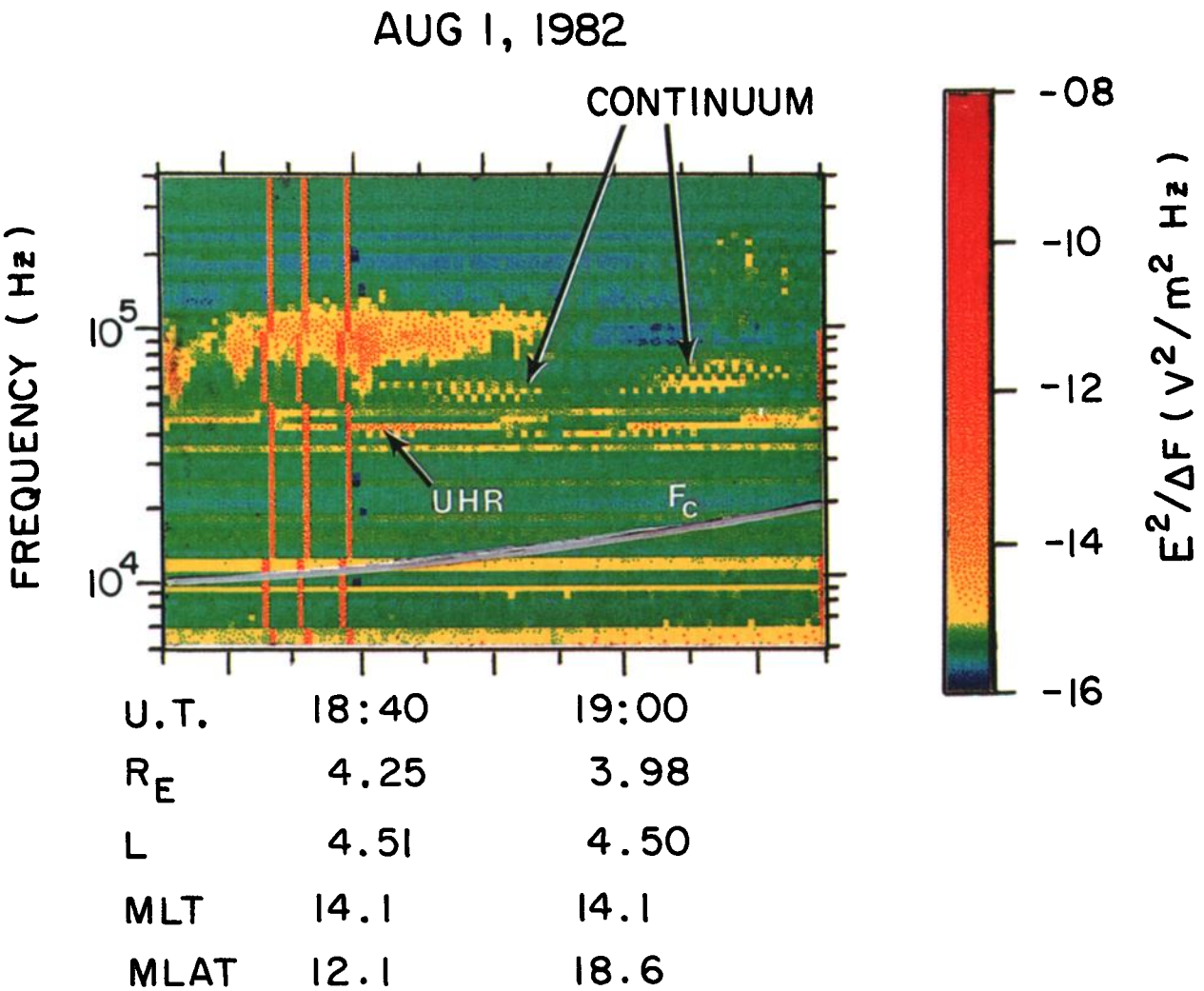

Plate 5. Spectrogram of continuum event of August 1, 1982. Note the low-frequency tail of AKR at 1840 UT that appears to be associated with the continuum radiation.

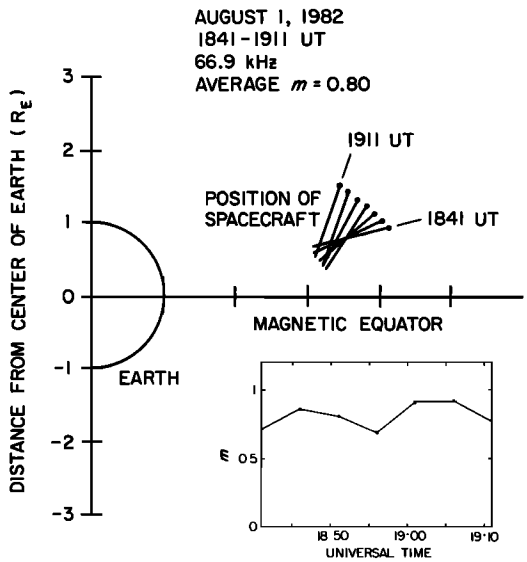

Fig. 19. Direction-finding result for the continuum radiation event shown in Plate 5.

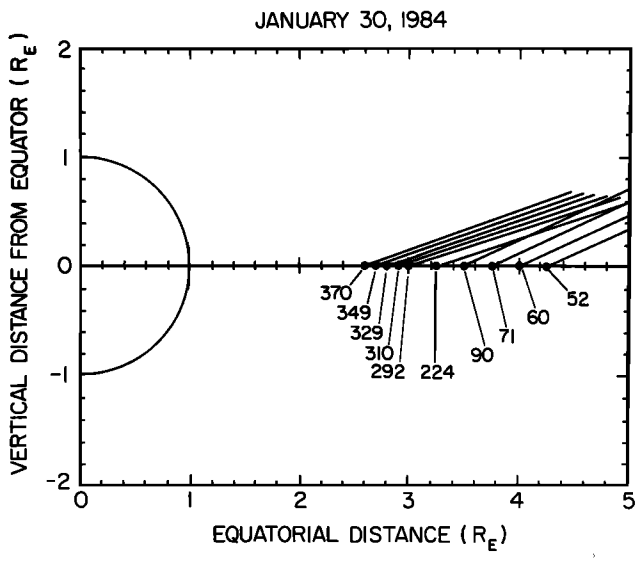

Fig. 20. Directions of arrival predicted from equation (1) based on an independently derived model of the electron density. Dots indicate the modeled source positions. The number associated with each dot is the predicted frequency of continuum radiation emission from that point.

inspection of the data. Most spectrograms display significant asymmetry. In fact, all of the individual cases studied in section 6 show asymmetry in the direction-of-arrival pattern except for that of February 23, 1982, for which the data are not of sufficient duration to indicate symmetry. Some of this asymmetry is clearly related to the orbit, as in the case of April 19, 1982 (Plate 1), where the continuum event appears to turn on abruptly at 0650 UT when the spacecraft was at around 4.1 R_E geocentric distance and $-4°$ magnetic latitude. The drop in f_{UHR} at this time indicates that the spacecraft is crossing the plasmapause and emerging into a region where the radiation can be detected. The January 30, 1984, event also shows some asymmetry which is probably orbit related. The emission has a slight upward frequency trend which corresponds to the movement of the spacecraft toward the Earth. The same trend is evident in the brightest component of the event of April 4, 1984, and in the August 1, 1982, event. This trend is also visible in the March 2, 1982, event reported by *Gurnett et al.* [1988]. In this paper, Gurnett et al. speculate that the frequency change was due to the radiation source moving as the spacecraft crossed the magnetic equator. However, the variations in frequency with changes in the geocentric distance of the spacecraft are too common to be coincidence. In fact, apparent source motion as the spacecraft crosses the magnetic equator is observed in the January 30, 1984, event in this study (see Figure 13). The apparent asymmetry of continuum events appears to be related to the orbit configuration, although another possibility is that the magnetic field or electron density is asymmetric about the equator.

The statistical data bear out this conclusion. Figure 7, the scatterplot of spectral density against propagation angle from the magnetic equator, shows no trend. Figure 8 shows a basically flat occurrence distribution over angle from the magnetic equator. Over the 75 events in these statistical

TABLE 1. Comparison of Calculated Plasma Frequency at Source With Observed Frequency of Radiation

Date	Time, UT	Frequency, kHz	Position of Source on Magnetic Equator, R_E	Predicted Angle From Magnetic Equator, deg	Measured Angle From Magnetic Equator, deg
Feb. 23, 1982	1950–2015	36.1–38.6	3.6	35°	48°–62°
		41.1–51.2	3.1–3.3	36°–38°	41°–49°
		58.0–71.4	2.0–2.8	38°–52°	32°
April 19, 1982	0830–0845	90.0–99.2	2.8	33°	43°–50°
	0735–0830	133.6–138.6	2.8–3.0	25°–30°	18°–42°
Jan. 30–31, 1984	2320–0005	44.6	3.6–3.7	32°–33°	56°–63°
	2315–2355	58.0–89.8	3.2–3.3	30°–31°	38°–50°
		133.6–154.2	2.8–3.0	31°–34°	37°–58°
April 4–5, 1984	2320–0010	71.4	2.3–3.2	31°–45°	46°–53°
	0025–0035				20°–21°
	0100–0120				27°–52°
March 2, 1982	1505–1535	95	2.7–3.0	30°–34°	10°–50°
	1550–1605	70	3.5–3.7	26°–28°	15°–29°

studies, continuum radiation appears to be emitted symmetrically with respect to the magnetic equator.

The radio window hypothesis requires not only that the pattern of continuum radiation be symmetric but that it consist of two distinct beams, one on each side of the magnetic equator. As in the case of symmetry, the dual-beam hypothesis of beaming is not confirmed by simply looking at spectrograms of continuum radiation. For example, the April 19, 1982, event is continuously observed over a large range of spacecraft positions. The January 30, 1984, event, between 60 and 90 kHz, shows a hint of a minimum around the magnetic equator crossing, although the intensity does not fall off by orders of magnitude as it should according to the radio window hypothesis. The highest-frequency emission, which is very faint, appears to show a real beaming effect. The event of August 1, 1982, seems to have two distinct beams, but the event is away from the magnetic equator and is therefore generally different in character from the other events. The very intense component of the April 4, 1984, event is continuous across the equator crossing. However, the component between 50 and 100 kHz and between 2325 and 0010 UT looks as if it might be a beamed emission. Thus the data seem to indicate that continuum radiation is beamed only some of the time. It is necessary to resort to the statistical evidence to establish whether continuum radiation is beamed.

The statistical evidence, shown in Figures 7 and 8, shows continuous distributions in both intensity and occurrence out to 40°–60° from the magnetic equator. As predicted from observed source positions and frequencies, the outer limit on beaming angle is reasonable, although it does not agree with the prediction based on the electron density model, as shown in Figure 20. However, the inner limit of both sets of predictions is not observed at all. There ought to be a minimum in both occurrence and intensity between −20° and +20° if the radio window hypothesis is true. A minimum of this extent is not observed.

This lack of an observed minimum around the magnetic equator is probably the strongest evidence against the radio window model that is presented in this study. However, there is other evidence worth discussing.

The beaming angle predictions based on specific electron densities give fairly constant and low beaming angles, around 20° from the magnetic equator. Very clearly, the angular spread of the radiation does not conform to this prediction. In fact, most of the direction-finding diagrams show a wide angular spread. There are a large number of beaming angle observations that are well away from the predictions of equation (1) in conjunction with independent electron density models.

Table 1 reinforces this result. Without using electron densities, this table shows that (1) does not give consistent results when radiation frequencies and source positions from the direction-finding diagrams are used to calculate the predicted beaming angle. The table shows that calculated results are usually either lower or higher than the actual beaming angle. From this admittedly small sample it appears that the greatest errors occur at low frequencies where the source position is often best defined (see, for example, Figures 9 and 12).

Thus there is strong evidence in the observed beaming pattern against the radio window hypothesis. Unfortunately, the evidence is not perfect. Some of the problems are noted below.

It has been noted in the discussion of the spectrograms that an intensity minimum is indeed sometimes visible. The case of January 30, 1984, between 50 and 100 kHz, shows a minimum in the radiation intensity in a range around the equator, although the intensity does not fall off by the 20 dB predicted by *Budden and Jones* [1987]. The upper frequency band shows the radiation going to background around the equator. The event of August 1, 1982 (Plate 5), shows the radiation going to background between two beams, although the source of radiation does not appear to be at the equator. The location of observed minima at the equator is consistent with the radio window hypothesis.

The statistical studies of section 4 are based on the assumption that the source of radiation is very near the magnetic equator. This appears to be a reasonable assumption, and yet it may not always be true. In addition to the August 1, 1982, event, the middle frequency band of the event of April 19, 1982, has a direction-of-arrival pattern, shown in Figure 9, that indicates that the source may be spread out along a magnetic field line with perhaps a stronger component at the equator. A related possibility that may account for the lack of statistically detectable beaming is that of a time variable source position. If the source varies its latitudinal position, it would cause the distributions in occurrence and intensity expected from the radio window model to be smeared out, probably something like what is seen in Figures 6 and 7.

Horne [1989] has pointed out that within the context of the radio window model, continuum radiation emitted from radio windows near the equator is expected to have higher intensity than that emitted at higher latitudes. The very faint occurrence gap observed at the equator at high intensities in Figure 7 and mentioned in section 5 could be the result of such an effect. If this faint occurrence gap is real, it lends some support to the idea of latitudinally extended or variable radio windows. However, often the radiation observed at the equator is of a different character from continuum. Sometimes it takes on the appearance of $(n + 1/2)f_{ce}$ modes as in Plate 4. Quite often spin modulation analysis results in a large error, which means these time intervals will not be counted in the statistics. This is the probable explanation of this occurrence gap.

Thus variable and extended sources go some distance toward explaining differences with the radio window model. However, such mechanisms do not account for individual cases such as the lowest frequency band of the April 19, 1982, event, where a single well-defined point source gives a direction-of-arrival pattern with a wide angular distribution and a very small intensity minimum near the equator.

Another problem with the interpretation of the data that weakens the conclusion of this study is the fact that there is a weak spin-modulated radiation, probably from the Sun, that influences the direction-finding results at high frequencies some of the time. This radiation is visible over a very wide frequency range in Plate 2, the spectrogram for the January 30, 1984, event. The effect of this type of radiation would be expected to be what is observed in Plate 3; the pattern of Figure 14 is reproduced except that the beaming angle from the magnetic equator is sharply reduced. In general, this helps to explain the directions of arrival close to the magnetic equator but makes it harder to explain the large

angles found, particularly when compared to the results using the electron densities.

One aspect of continuum radiation which might be partially explicable within the framework of the radio window hypothesis is the appearance of several bands of radiation at widely varying frequencies. Of the case studies presented, all except that of August 1, 1982, appear to be multibanded. Figure 20 illustrates that with realistic electron densities used in equation (1), it is possible for ray paths from regions of different plasma frequencies to cross, enabling the spacecraft to detect two or more bands at once. The trend illustrated here conforms with the results of direction finding in that higher frequencies appear to be radiated at lower beaming angles. In detail, however, Figure 20 does not agree well with the observed event of January 30, 1984. The actual event shows three bands of continuum radiation while the diagram based on the electron density shows the possibility of two bands only. Also, sources of the different frequencies do not agree with the source positions observed in the direction-finding diagrams. for example, the source at 44 kHz would appear to come from about 4.5 R_E in Figure 20, whereas the direction-finding diagram shows it to be inside 4.0 R_E.

Another effect that this type of analysis could help to explain is the bandwidth. It is observed that almost all continuum radiation events have observably finite bandwidths. A source extended radially along the magnetic equator would cover a wide range of plasma frequencies. Figure 20 shows that these frequencies would have a very nearly constant beaming angle. In the case of the January 30, 1984, event the middle frequency band, between 60 and 90 kHz, appears to come from a region along the magnetic equator between 2.8 and 3.0 R_E. Figure 20 shows that this radiation is emitted over a wide range of geocentric distance, between 3.5 and 4.0 R_E. While the mechanism for explaining the bandwidth exists, the details again do not appear to agree with predictions of the radio window model.

Finally, the radio window hypothesis specifically predicts that one source region will emit at a single frequency in one direction. Figure 20 illustrates this point for a series of source points along the magnetic equator. Figure 18, the direction-finding diagram for the strong event of April 4, 1984, shows three quite distinct beaming angles at a single frequency and apparently from a single region along the magnetic equator between radii of 2.5 and 3.0 R_E. If the source is on the magnetic equator, this is a clear contradiction of the radio window hypothesis. A way out for the hypothesis might be if there were a number of sources extended latitudinally along L shells. Lower-angle emissions, from lower L shells, could be detected in the equatorial intensity minimum of the emissions from sources at higher L values.

To sum up the results of this study, it has been seen that there is very little positive evidence for the radio window hypothesis for the generation of continuum radiation. Some of the observations can be qualitatively explained by resorting to the inherent complexity of the geometry of the radiating region. However, with all of this complexity, one still expects that if the radio window model were true, a minimum in the intensity should be observed around the magnetic equator and maxima should be observed close to 20° north and south of the equator. These features are not consistently or clearly observed in either the statistical data or the individual case studies. The correctness of the radio window hypothesis will be established by the ability to model a source region that can emit over a wide range of angles from the plane of the magnetic equator both statistically and in individual cases.

Acknowledgments. We would like to acknowledge computing support from Terry Averkamp and Bob Lane, and discussions of the instrumentation as well as the phenomenon under investigation with Rich Huff. Thanks to Rich also for pointing out the possible connecting of AKR with continuum radiation in the August 1, 1982, event and to Roger Anderson for supplying electron density models. This work was supported by grant NAG5-310 with Goddard Space Flight Center, and grant NAGW-1488 with NASA Headquarters.

The Editor thanks R. B. Horne and W. Calvert for their assistance in evaluating this paper.

REFERENCES

Ashour-Abdalla, M., and H. Okuda, Generation of ordinary mode electromagnetic radiation near the upper hybrid frequency in the magnetosphere, *J. Geophys. Res.*, *89*, 9125, 1984.

Baumback, M. M., Direction-finding measurements of type III radio bursts out of the ecliptic plane, M.S. thesis, Univ. of Iowa, Iowa City, 1976.

Brown, L. W., The galactic radio spectrum between 130 and 2600 kHz, *Astrophys. J.*, *180*, 359, 1973

Budden, K. G., The theory of radio windows in the ionosphere and magnetosphere, *J. Atoms. Terr. Phys.*, *42*, 287, 1980.

Budden K. G., *The Propagation of Radio Waves: The Theory of Radio Waves of Low Power in the Ionosphere and Magnetosphere*, Cambridge University Press, New York, 1985.

Budden, K. G., and D. Jones, Conversion of electrostatic upper hybrid emissions to electromagnetic O and X mode wave in the Earth's magnetosphere, *Ann. Geophys., Ser. A*, *5*, 21, 1987.

Filbert, P. C., and P. J. Kellogg, Observations of low-frequency radio emissions in the Earth's magnetosphere, *J. Geophys. Res.*, *94*, 8867, 1989.

Gurnett, D. A., The Earth as a radio source: The nonthermal continuum, *J. Geophys. Res.*, *80*, 2751, 1975.

Gurnett, D. A., and L. A. Frank, Continuum radiation associated with low-energy electrons in the outer radiation zone, *J. Geophys. Res.*, *81*, 3875, 1976.

Gurnett, D. A., and R. R. Shaw, Electromagnetic radiation trapped in the magnetosphere above the plasma frequency, *J. Geophys. Res.*, *78*, 8136, 1973.

Gurnett, D. A., W. Calvert, R. L. Huff, D. Jones, and M. Sugiura, The polarization of escaping terrestrial continuum radiation. *J. Geophys. Res.*, *93*, 12,817, 1988.

Hoffman, R. A., and E. R. Schmerling, Dynamics Explorer program: An overview, in *Dynamics Explorer*, edited by R. A. Hoffman, p. 345, D. Reidel, Norwell, Mass., 1981.

Horne, R. B., Path-integrated growth of electrostatic waves: The generation of terrestrial myriametric radiation, *J. Geophys. Res.*, *94*, 8895, 1989.

Horne, R. B., Narrow-band structure and amplitude of terrestrial myriametric radiation, *J. Geophys. Res.*, *95*, 3925, 1990.

Jones, D., Source of terrestrial non-thermal radiation, *Nature*, *260*, 686, 1976.

Jones, D., Latitudinal beaming of planetary radio emissions, *Nature*, *288*, 225, 1980.

Jones, D., Radio wave emission from the Io torus, *Adv. Space Res.*, *1*, 333, 1981.

Jones, D., Terrestrial myriametric radiation from the Earth's plasmapause, *Planet. Space Sci.*, *30*, 399, 1982.

Jones, D., The magnetopause as a source of nonthermal continuum radiation, *Phys. Scr.*, *35*, 887, 1987.

Jones, D., Planetary radio emissions from low magnetic latitudes: Observations and theories, in *Planetary Radio Emissions II*, edited by H. O. Rucker, S. J. Bauer, and B. M. Pederson, pp. 256–293, Österreichische Akademie der Wissenschaften, Graz, Austria, 1988.

Jones, D., W. Calvert, D. A. Gurnett, and R. L. Huff, Observed

beaming of terrestrial myriametric radiation, *Nature*, *328*, 391, 1987.

Kurth, W. S., Detailed observations of the source of terrestrial narrowband electromagnetic radiation, *Geophys. Res. Lett.*, *9*(12), 1341, 1982.

Kurth, W. S., M. M. Baumback, and D. A. Gurnett, Direction-finding measurements of auroral kilometric radiation, *J. Geophys. Res.*, *80*, 2764, 1975.

Kurth, W. S., D. A. Gurnett, and R. R. Anderson, Escaping nonthermal continuum radiation, *J. Geophys. Res.*, *86*, 5519, 1981.

Lembege, B., and D. Jones, Propagation of electrostatic upper hybrid emission and *Z* mode waves at the geomagnetic equatorial plasmapause, *J. Geophys. Res.*, *87*, 6187, 1982.

Melrose, D. B., A theory for the nonthermal radio continua in the terrestrial and Jovian magnetospheres, *J. Geophys. Res.*, *86*, 30, 1981.

Murtaza, G., and P. K. Shukla, Nonlinear generation of electromagnetic waves in a magnetoplasma, *J. Plasma Phys.*, *31*, 423, 1984.

Okuda, H., M. Ashour-Abdalla, M. S. Chance, and W. S. Kurth, Generation of nonthermal continuum radiation in the magnetosphere, *J. Geophys. Res.*, *87*, 10,457, 1982.

Rönnmark, K., Emission of myriametric radiation by coalescence of upper hybrid waves with low-frequency waves, *Ann. Geophys.*, *1*, 187, 1983.

Rönnmark, K., Myriametric radiation and the efficiency of linear mode conversion. *Geophys. Res. Lett.*, *16*, 731, 1989.

Shawhan, S. D., D. A. Gurnett, D. L. Odem, R. A. Helliwell, and C. G. Park, The plasma wave and quasi-static electric field instrument (PWI) for Dynamics Explorer-A, in *Dynamics Explorer*, edited by R. A. Hoffman, p. 535, D. Reidel, Norwell, Mass., 1981.

Steinberg, J. L., and S. Hoang, Electric noise observations with the ISEE-3 radio receiver: Thermal noise and the $2f_p$ line from the Lagrange point to 14 R_E from the Earth, *Ann. Geophys., Ser. A*, *4*, 429, 1986.

D. A. Gurnett and D. D. Morgan, Department of Physics and Astronomy, University of Iowa, Iowa City, IA 52242.

(Received July 17, 1990;
revised January 23, 1991;
accepted January 24, 1991.)